Curve normalization for shape retrieval

Nacéra Laiche *, Slimane Larabi, Farouk Ladraa, Abdelnour Khadraoui

Computer Science Department, University of Sciences and Technology, Houari Boumediene, Algiers, Algeria

ARTICLE INFO

ABSTRACT

In this paper, we propose a novel part-based approach for two dimensional (2-D) shape description and recognition. According to this method, first the polygonal approximation is employed to represent the outline shape by an ordered sequence of parts. Then using the Least squares model, each part is associated with a cubic polynomial curve. The obtained curves are normalized that are invariant to scaling, rotation and translation. Finally, based on shape similarity of resulting curves, a shape similarity between an input shape and its reference model is defined. A two-step matching algorithm is proposed. Experiments using several benchmark databases are performed and the obtained retrieval results demonstrate that the proposed approach is effective as compared to other matching techniques.

1. Introduction

Shape recognition is a very important application area in computer vision and in multimedia processing particularly. But building a shape retrieval process requires two important components: a shape representation and a matching algorithm. A good shape matching should be invariant to affine transformations such as translation, scaling and rotation. Based on the silhouette of objects, various descriptors and matching algorithms have been proposed during the past decades [1]. The proposed methods are based on statistical approaches which use global features extracted from the shape like moments [2,3] and Fourier descriptors [4,5], local structural features such as segments and arcs [6,7] and part decomposition [8]. There are also hybrid approaches that combine both local and global shape features such as rolling penetrate descriptor [9,10].

Since the global shape features have some limitations in shape representation and poor performance in matching shapes partially occluded, we propose in this paper two new approaches: these are part-based representation and matching method. The part-based silhouette representation we use is built only on curves. Boundary shape is decomposed into different parts with associated least squares curves. The shape matching task is divided into two steps: the first step consists in reducing the search space by using global features such as invariant moments of order two. The second one is based on the similarity between normalized curves.

The rest of this paper is organized as follows. In Section 2, a brief review of shape representation and matching methods is presented. In Section 3, details on the proposed approach of shape representation are described. The associated shape matching process based on the defined similarity measure is presented in Section 4. Section 5 presents the evaluation of the approach and a comparative study with some existing methods of the state of the art. Finally, Section 6 gives some conclusions and concludes the paper.

2. Related work

Numerous techniques and algorithms have been proposed in the literature to represent objects based on their

---

* Corresponding author.
  E-mail addresses: nlaiche@usthb.dz (N. Laiche),
slarabi@usthb.dz (S. Larabi).

silhouettes. There are mainly two-kinds of methods: surface-based and contour-based methods. In general, surface-based methods extract features from the whole shape region. Some methods in this kind are Zernike moments [11,12] and Legendre moments [13,14] which have demonstrated to achieve excellent performance but these methods are not suitable for object recognition in the presence of occlusion. Generic Fourier descriptor [15] is another well known shape descriptor which uses the property of Fourier transform and allows multi-resolution analysis. The authors in [16] proposed another way to describe shapes using the PCA- based methods. On the other hand, the contour-based methods explore boundary shape information. They are more complicated and requiring sophisticated implementations but they are more suitable than global methods for recognizing partially visible objects. In this category we find chain codes which consist of line segments that must lie on a fixed grid with a fixed set of possible orientations [17], polygonal approximation [18,19] and skeleton approach. In polygonal approximation approach, a shape is decomposed into line segments. The polygon vertices are used as primitives and then some features are extracted for each primitive. The median axis transformation or skeleton is introduced by Blum in [20]. It consists to reduce regions to curves that follow the global shape of an object. Later Sebastian et al. [21] used this descriptor for shape recognition. Petrakis and Milios [22] propose to represent shapes as a collection of segments between two consecutive inflexion points. The obtained segments are considered at different levels of shape resolution.

The goal of the above references is to approximate a shape as a polygon and then the shape is represented by a set of line segments. This description work well for man-made objects but it is not suitable for natural objects [1].

Mokhtarian et al. [23] proposed the Curvature Scale Space (CSS) descriptor, which is based on the maxima of the curvature zero-crossing boundaries to represent shapes. CSS representation is invariant under the affine transformations but it is sensitive to occlusion and convex shapes [24]. Recently Fotopoulou and Economou [25] proposed a multi-scale descriptor, which is based on the sequence of angles formed by the boundary points and then computed at different scales. Triangle area representation (TAR) [26] is another type of multi-scale descriptors based on the signed areas of triangles formed by boundary points at different scales. Other techniques consist of approximate the shape contour by differential-Turning Angle Scale Space function (d-TASS) [27,28], B-splines [29,30] and height functions [31,32]. The height function for one sample point is defined by distances of all the other sample points to its tangent line. The obtained height functions are then smoothed to represent and recognize 2D objects silhouettes.

Shape context (SC) [33] is a method for finding corresponding between point sets. Based on the inner distance, SC is extended to Inner-Distance Shape Context (IDSC) [34]. SC and IDSC have the ability to extract very discriminative features for a shape and to deal with the inexact correspondence problem in shape matching. However, they are sensitive to different shape poses and deformations.

Recently, the authors in [35] presented a novel shape representation based on the local phase quantization. It transforms the descriptors obtained by the inner distance shape context, shape context and height functions into a matrix descriptor using the local phase quantization descriptor. The extracted matrix descriptors are then compared with the Jeffry distance. Later Hu et al. [36] proposed a novel contour-based hand shape recognition method called Coherent Distance Shape Contexts (CDSC), which is based on shape context and Inner-distance shape context. This descriptor is robust to hand poses and can be used in both hand shape and palmprint recognitions. Another interesting technique for two-dimensional shape matching, called contour flexibility is developed by Xu et al. [37] in which the deformable potential at each point of boundary is represented.

Shapes can also be modeled using part-based representation which has played an important role in object recognition. Organizing shape representations in terms of parts allows one to separate the representation of the shape of each individual part from the representation of the spatial relationships between the parts. This, in turn, leads to a more robust representation of shape. In [38] shapes are decomposed into different rectangles. The locations of the rectangles and their dimensions are selected by using a dynamic programming. The authors in [39] propose the use of the curvature zero-crossing points from a smoothed contour to get the parts, called tokens. The orientations and the maximum curvatures of the obtained parts are taken into account to represent shapes and matching. The method is not invariant to rotation because of the token orientation [40]. Using a dynamic programming, Latecki et al. [41] propose a method for partial shape matching, where local tangents to silhouettes are used for shape description. In [42] Cui et al. propose the use of the integral of absolute curvature as shape descriptor. For matching parts of occurring curves, they use the normalized cross correlation. The method is invariant to rotation, scale and translation. Daliri and Torre [46] proposed a representation for shape-based recognition based on the extraction of the perceptually relevant fragments. According to this approach, each shape is transformed into a symbolic representation, using a predefined dictionary for the contour fragments, which is mapped to an invariant high-dimensional space that is used for recognition.

In this paper, we explore a different approach to object recognition which is based on the analysis of the boundary of the shape using normalized curves. The proposed approach combines the advantages of polygonal approximation that are suitable for shape partitioning as its vertices correspond to high curvature points of the shape boundary and the least squares model that is particularly suitable for minimizing quadratic errors. The representation of the two-dimensional curve normalization for shape-based retrieval is proposed instead of line segments because segments are useful for man-made objects but they are not suitable if a shape consists of a curved boundary. The proposed approach involves three major steps: first, the extraction of the meaningful parts constituting the boundary shape, secondly, the modeling of the extracted part using the

least squares approximation, and finally the descriptor matching step.

The main contributions of this paper are the following:

(1) Detection of significant boundary parts. In partitioning a shape boundary, we have used the concave points extracted from the boundary using the vertices of its polygonal approximation. These points are those where two adjoining parts meet.
(2) The possibility of exploring the least squares model to shape representation and recognition. Each part is associated with its cubic least squares curve. A shape is then presented as a set of normalized boundary curves vector.
(3) Exploiting the proposed matching algorithm for contour parts (normalized least squares curves) similarity to establish full shape similarity. This is achieved by identifying the similar curves between two shapes.
(4) The ability of the proposed approach for curve similarity to match shapes under occlusions.

3. Shape modeling

In this section, we propose the steps allowing the representation of the shape using the polygonal approximation and the least squares model.

3.1. Extraction of contour parts

High curvature points are effective features for shape representation, reflecting the concave and convex parts of a shape. The proposed decomposition process is based on concave points of shapes which can be estimated by curvature. Selecting concave points as the decomposition points allows the extracting of the meaningful parts of shapes. Fig. 1 illustrates an example of shape partition for a shape dog.

Concave points are located on the boundary using the polygonal approximation [44]. The concave polygon vertices are used as boundaries between parts. The whole algorithm for the decomposition can be summarized as follows:

– Detect the high curvature points which are defined as the vertices of the polygon with specified parameter.
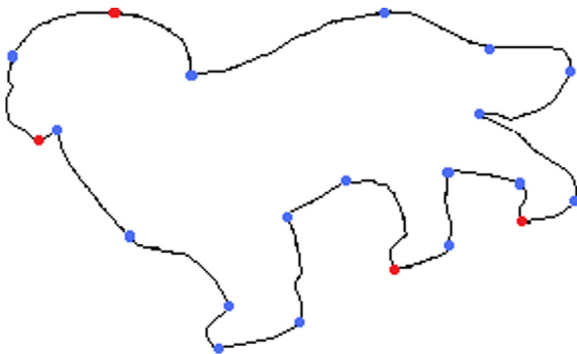
Fig. 1. Shape partition into parts.

– Select the concave vertices of the polygon and then discard the redundant ones that are in the consecutive points.
– Associate concavity measurement at each concave vertex as the ratio r/d where r is the distance from the concave vertex to associated chord of length d.
– Finally, select only the concave vertices of high degree of concavity from the remaining points in order to decompose the boundary into meaningful parts, which are defined as boundary curves between each pair of the concave vertices.

3.2. Least Squares curve modeling

In the following, it is assumed that the shape boundary of an object is represented by a set of ordered parts. The least squares model is used to modelize each part by a cubic polynomial curve. All the curves are given relatively to the minimum area rectangle MAR including the shape (see Fig. 2).

The MAR associated to a shape is defined as the smallest rectangle minimizing the area between it and the convex hull enclosing the shape [45]. For each shape, a unique convex hull is associated. In the same way, the MAR is unique for each shape. Changing the orientation of a shape will change also the orientation of the MAR, but its dimensions remain unchanged.

Any cubic least squares curve yields a set of critical points extracted from the discrete curve. These points are considered as approximation points. To select them and to ensure that the chosen points can provide a best approximation, a simple strategy is implemented:

– Input boundary shape and the corresponding parts set $\{P_i\}$.
– Compute the length of each part P_i and define the shortest one as distance threshold D_{th}.
– If part length L_i is between D_{th} and $2D_{th}$ then the part is approximated by 1 equally spaced points taken from the part.
– For part length between $2D_{th}$ and $6D_{th}$, the approximation points are 3 spaced.
– If the length L_i is greatest than $6D_{th}$, then the part is represented by 4 equally spaced points.

After the selection of the approximation points, the least squares model is used to model each part P_i by a cubic polynomial curve $P_i(x)$. The curve is defined by

$$P_i(x) = \sum_{k=0}^{3} b_k x^k, \tag{1}$$

where b_k; $k = 0, 1, 2, 3$ are the polynomial factors.

The goal is to specify the polynomial factors b_k; $k = 0, 1, 2, 3$ in such a way that minimizing the distance between the boundary part of shape and its least squared curve representation

$$G(b_0, b_1, b_2, b_3) = Min_{P_i} \left\{ \sum_{j=1}^{m} |P_i(x'_j) - y'_j|^2 \right\}, \tag{2}$$
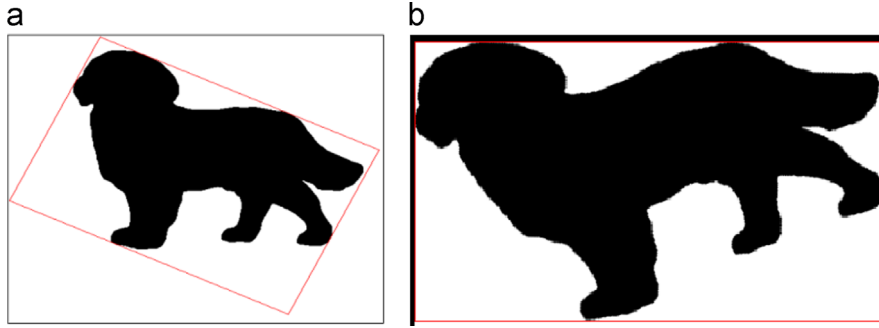
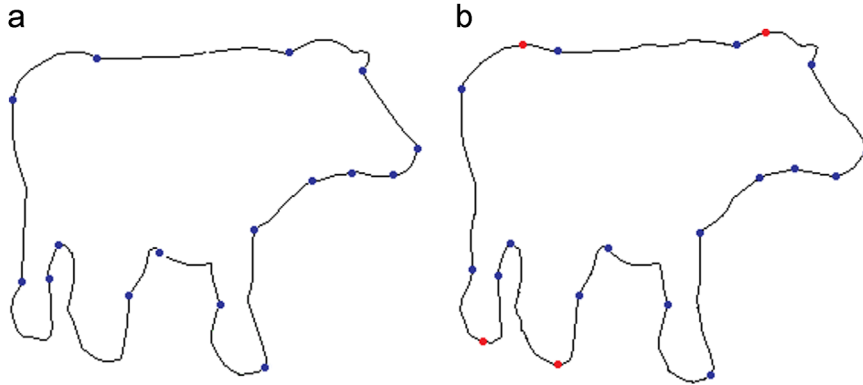**Fig. 2.** The minimum rectangle MR including the shape.

Fig. 3. (a) Shape decomposition into parts and (b) Visualization of the new decomposition points.

The points (x'_j, y'_j), $j = 1, 2, \ldots, m$ denote the m approximation points of the elementary curve P_i of the boundary contour used for the least squares curve $P_i(x)$.

The coordinates (b_0, b_1, b_2, b_3) can be obtained using partial derivatives equations and the Householder factorization algorithm for the matrix arising from the application of the least squares model. From Eqs. (1) and (2), the following system can be written as:

$$\nabla G = 0 \Leftrightarrow \begin{cases} \frac{\partial G}{\partial b_0} = 0 \\ \frac{\partial G}{\partial b_1} = 0 \\ \frac{\partial G}{\partial b_2} = 0 \\ \frac{\partial G}{\partial b_3} = 0 \end{cases} \tag{3}$$

The solution for the parameters (b_0, b_1, b_2, b_3) is then given in matrix form as $A = D^T D B$,

where A and B are of size 4×1 containing the given data and the polynomial factors respectively: $a_i = \sum_{j=1}^{m} y'_j x'^i_j$, $i = 0, 1, 2, 3$. The $m \times 4$ matrix D contains the powers of x'_i as shown below

$$D = \begin{pmatrix} 1 & x'_0 & x'^2_0 & x'^3_0 \\ 1 & x'_1 & x'^2_1 & x'^3_1 \\ . & . & . & . \\ . & . & . & . \\ . & . & . & . \\ 1 & x'_m & x'^2_m & x'^3_m \end{pmatrix}, \quad B = \begin{pmatrix} b_0 \\ b_1 \\ b_2 \\ b_3 \end{pmatrix}, \quad A = \begin{pmatrix} \sum_{j=1}^{m} y'_j \\ \sum_{j=1}^{m} y'_j x'_j \\ \sum_{j=1}^{m} y'_j x'^2_j \\ \sum_{j=1}^{m} y'_j x'^3_j \end{pmatrix}$$

In the practical modeling application, we have to deal with the parts that have many points with the same abscissa, as shown in Fig. 3(a). For these parts, the least squares model will get fail. To address this problem, new decomposition points will be located to segment these parts. An example of this case is shown in Fig. 3(b). The red circles illustrate the new decomposition points on the parts in question. In Fig. 3 (a), the blue points illustrate the concave vertices which are used to decompose the original boundary shape into parts

3.3. Curves normalization

Translation invariance is used as the first stage of normalization. Invariance to rotation is ensured using the MAR. The MAR of shapes are adjusted such as the length of the rectangle coincides with the Y-axis of the image and its width with the X-axis. To achieve invariance to scale change for the curves, we carry-out a transformation on the obtained least squares curves. Let $P_i = \{X_1 = (x_1, P_i(x_1)), \ldots, X_n = (x_n, P_i(x_n))\}$ be n curve points obtained through the least squares approximation of the part P_i, where $P_i(x)$ represents the cubic least squares curve associated to the part P_i. The transformation is defined by mapping each point X_i to $X'_i = (x_i/Max, P_i(x_i)/Max)$ for $i = 1, 2, \ldots, n$. Max represents the maximal distance from the centroid to the boundary shape.

4. Shape matching

Matching between query shapes and models is achieved by comparing their features. The features in our

approach are related to the second order of geometric moments and the normalized curves.

4.1. First search

Due to the size of the database of normalized curves, for a given query shape, we first reduce the search space. Then a detailed measure of match is computed only on the corresponding shapes. The $p+q$ order normalized moments of order up to 2 are taken into account for reducing the search space

$$M_{pq} = \frac{1}{M_{00}} \sum_x \sum_y (x-x_G)^p(y-y_G)^q f(x,y) \qquad (4)$$

where the area of a shape is M_{00}, (x_G, y_G) is the shape's centroid and $f(x,y)$ is the mass distribution of the object.

Based on this, the followed procedure is performed: given two global parameters I_1 and I_2, a threshold ε is set so that all models satisfying $I_1 \le \varepsilon$ and $I_2 \le \varepsilon$ are discarded.

The two parameters are defined such as

$$I_1 = \begin{cases} \left(\frac{L'}{L}\right)\left(\frac{M_{20}}{M'_{20}}\right) & if : L \prec L' \\ \left(\frac{L}{L'}\right)\left(\frac{M'_{20}}{M_{20}}\right) & otherwise \end{cases}, \qquad (5)$$

$$I_2 = \begin{cases} \left(\frac{L'}{L}\right)\left(\frac{M_{02}}{M'_{02}}\right) & if : L \prec L' \\ \left(\frac{L}{L'}\right)\left(\frac{M'_{02}}{M_{02}}\right) & otherwise \end{cases}, \qquad (6)$$

where L (resp. L') represents the arc length of the query shape (resp. model shape).

(M_{02}, M_{20}) and (M'_{20}, M'_{20}) are the moments of order 2 of the query and the model shape respectively.

Then we define the similarity measure between the query and the selected models shapes, represented by their normalized curves.

4.2. Shape similarity

In the sequel, the process of shapes matching using their least squares curves representation is addressed. Two shapes are considered similar if they share similar curves according to an appropriate similarity measure.

4.2.1. Shape similarity of curves

Two normalized curves P and P' of a query shape Q and a reference shape M respectively are considered similar if the similarity measure defined below is under a threshold, otherwise they are different.

Let $\{a_1, a_2, \ldots, a_n\}$ and $\{b_1, b_2, \ldots, b_{n'}\}$ be the ordered points of the least squares curves constituting the curves P and P' respectively. The similarity between the two curves is defined as follows:

- For each point a_i of P, we compute $\min_{b_j \in P'} ||a_i - b_j||$, where $||.||$ is a norm defined on the point set of the curve such as the L_2 norm.
- Then we compute the distance from the curve P to the curve P' as the average of all the minimum distances
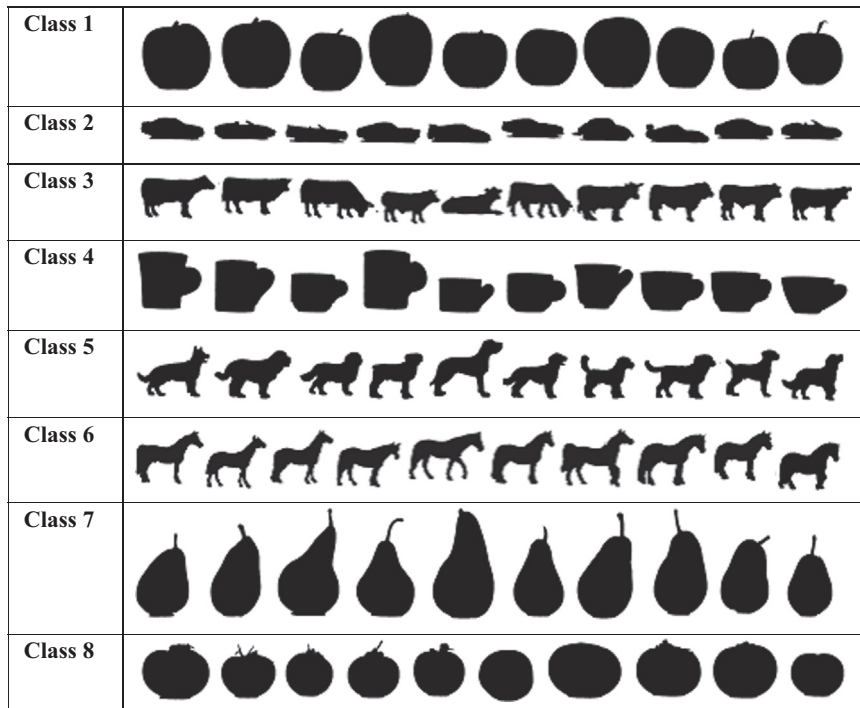
Fig. 4. ETH-80 database. Each row shows one category of object.

are computed previously

$$D_{P,P'} = \frac{1}{\text{length}(p)} \sum_{i=1}^{n} \min_{b_j \in P'} ||a_i - b_j||, \qquad (7)$$

where length (P) represents the length of curve P.
- In the same way, we compute

$$D_{P',P} = \frac{1}{\text{length}(P')} \sum_{i=1}^{n'} \min_{a_j \in P} ||b_i - a_j||, \qquad (8)$$

with length (P') is the length of curve P'.

The matching between the two normalized curves P and P' is valid when the values of the two distances $D_{P,P'}$ and $D_{P',P}$ are lower than the same threshold. This threshold is determined experimentally after several tests.
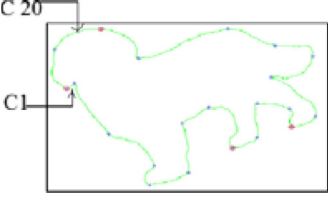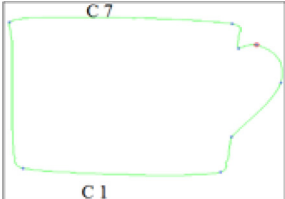
4.2.2. Computing shape similarity

Let $Q = {}^t(P_1, ..., P_r)$ be a given query shape and let $M = {}^t(P'_1, ..., P'_s)$ a model shape where $(P_i)_{i=1,...,r}$ and $(P'_i)_{i=1,...,s}$ represent the normalized curves corresponding, respectively, to query Q and model M. The similarity score between the two given shapes is defined by the number of similar curves as follows:

- The curves $P_1, ..., P_r$ are compared to the curves $P'_1, ..., P'_s$ according to their order using the measure similarity defined by the Eqs. (7) and (8).
- Count the number of similar curves.

Table 1
Shapes decomposition and their description.

Shape	Cubic Least squares curves
C 20 C1	$C_1(x) = -1447.19 + 2.57857*x + 0.0695954*x^2 - 0.000242569*x^3$. $C_2(x) = 876.911 - 11.5915*x + 0.0448752*x^2 - 5.43909.10^{-5}*x^3$. $C_3(x) = -17798.4 + 152.801*x - 0.43709*x^2 + 0.000417355*x^3$. $C_4(x) = 6151.13 - 35.2038*x + 0.0562573*x^2 - 1.59407.10^{-5}*x^3$. $C_5(x) = 12173.3 - 136.11*x + 0.475583*x^2 - 0.000529999*x^3$. $C_6(x) = -1814.76 + 17.1856*x - 0.0519636*x^2 + 5.2425.10^{-5}*x^3$. $C_7(x) = 522.114 - 4.93003*x + 0.0244665*x^2 - 4.5087.10^{-5}*x^3$. $C_8(x) = -11282 + 116.228*x - 0.39293*x^2 + 0.000441018*x^3$. $C_9(x) = -9519.84 + 70.767*x - 0.148647*x^2 + 6.8608.10^{-5}*x^3$. $C_{10}(x) = 3287.85 - 33.7869*x + 0.122035*x^2 - 0.000146316*x^3$. $C_{11}(x) = 8911.36 - 288.119*x + 1.87026*x^2 - 0.00342721*x^3$. $C_{12}(x) = 10139.5 - 110.819*x + 0.413135*x^2 - 0.000513266*x^3$. $C_{13}(x) = -7175.66 + 48.7412*x - 0.0536894*x^2 - 9.15724.10^{-5}*x^3$. $C_{14}(x) = 729.071 - 10.7925*x + 0.0615444*x^2 - 0.000103216*x^3$. $C_{15}(x) = 4826.74 - 82.718*x + 0.499673*x^2 - 0.00100576*x^3$. $C_{16}(x) = -20731.8 + 380.748*x - 2.29724*x^2 + 0.00461125*x^3$. $C_{17}(x) = -12054.3 + 273.345*x - 2.0443*x^2 + 0.00511877*x^3$. $C_{18}(x) = 5273.59 - 104.587*x + 0.710254*x^2 - 0.00163041*x^3$. $C_{19}(x) = -2947.79 + 56.346*x - 0.35856*x^2 + 0.000761607*x^3$. $C_{20}(x) = 13195.2 - 283.832*x + 2.02012*x^2 - 0.00479456*x^3$. $C_{21}(x) = -1946.28 + 31.7551*x - 0.182143*x^2 + 0.000345861*x^3$.
C 7 C 1	$C_1(x) = -25194.7 + 78.3124*x + 0.127583*x^2 - 0.000415294*x^3$. $C_2(x) = 3243.01 - 28.7585*x + 0.0931657*x^2 - 0.000100911*x^3$. $C_3(x) = -130.538 + 6.83213*x - 0.0297297*x^2 + 3.79181.10^{-5}*x^3$. $C_4(x) = -920.752 + 21.795*x - 0.123507*x^2 + 0.000232389*x^3$. $C_5(x) = 12483.8 - 230.523*x + 1.36477*x^2 - 0.00240672*x^3$. $C_6(x) = -969.334 + 35.9411*x - 0.338473*x^2 + 0.00105165*x^3$. $C_7(x) = -371938 + 14700.7*x - 193.411*x^2 + 0.84747*x^3$. $C_8(x) = -94.0353 + 0.51158*x - 0.00266919*x^2 + 4.4325.10^{-6}*x^3$.

- Compute the first score V_1 as the ratio

$$V_1 = \frac{N}{\min(r,s)}, \tag{9}$$

where N represents the number of similar curves between Q and M.

- We make a circular permutation on the index of the curves of the shape which has more curves, then we repeat the previous steps.
- After $(\max(r,s) - 1)$ permutations, the score $S(Q, M)$ between the query shape and the model shape is defined by

$$S(Q, M) = Max(V_1, \ldots, V_{Max\ (r,s)}), \tag{10}$$

where $V_1, V_2, \ldots$, and $V_{Max\ (r,s)}$ are the different scores computed at each step of comparison between the two sets of curves corresponding to Q and M.

5. Experimental results

In this section, we present some of our experimental results through several examples. Our approach is tested on standard shape matching databases used in a number of shape retrieval systems: the ETH-80, Kimia-99, Kimia-216 and MPEG-7 databases.

Queries	Retrieved Shapes						
	100%	100%	85%	75%	75%	62%	62%
	100%	81%	81%	81%	71%	66%	63%
	94%	80%	70%	62%	52%	47%	47%
	70%	63%	63 %	60%	54%	54%	54%
	65%	62%	61%	60%	57%	54%	52%
	77%	72%	61%	60%	55%	55%	50%
	100%	100%	100%	81%	81%	100%	77%
	86%	70%	68%	58%	54%	52%	50%
	78%	68%	62%	61%	53%	51%	46%
	100%	100%	100%	91%	85%	85%	78%

Fig. 5. Matching scores for some results.

5.1. ETH-80 database

The ETH-80 database contains eight classes of objects with ten objects per class [46]. Fig. 4 displays different shapes for each class. Each object is represented by some views spaced evenly over the upper viewing hemisphere. The shapes of the database are selected such that are significant in order to enable unambiguous evaluation.

The choice of the threshold values has an impact on the performance of the proposed retrieval approach. After several experiments, the combination of the values: $\varepsilon = 0.9$ for the first search and 0.15 for shape similarity of curves shows the best retrieval results.

5.1.1. Least squared curves

Table 1 presents two examples of shapes description and their associated least squares curves. Column 1

Fig. 6. Some example queries are shown in the left column with the most similar retrieved shapes for each one.

Fig. 7. Partial query shapes.
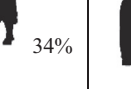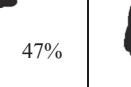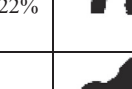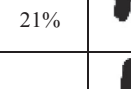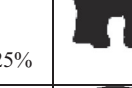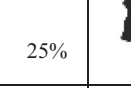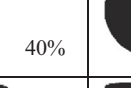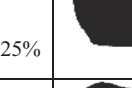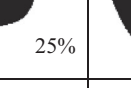
Fig. 8. The most similar shapes retrieved for each of the partial test queries.

Table 2
Recognition rates for some approaches for each category of object.

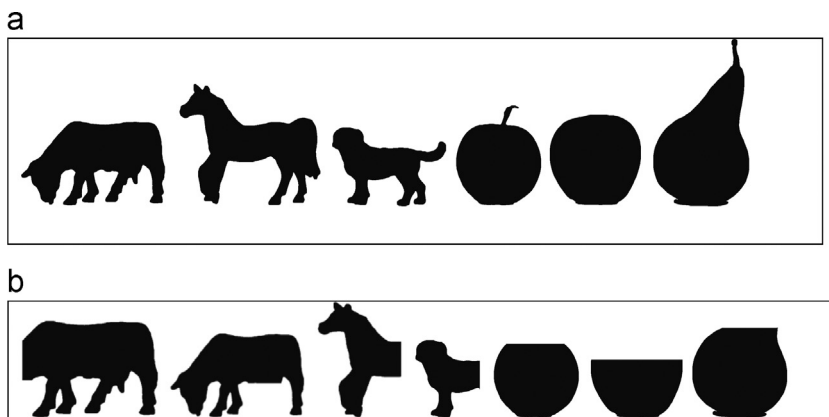| Approaches	Apple	Car	Cow	Cup	Dog	Horse	Pear	Tomato	Average
Robust Symbolic representation [43]	82.53	98.41	92.04	98.9	86.31	90.91	90.03	73.14	89.03
Cont greedy [46]	77.07	99.51	86.83	96.10	81.95	84.63	90.73	70.24	86.40
PCA masks [46]	88.29	100	75.12	96.10	72.20	77.80	99.51	67.80	83.41
PCA gray [46]	88.9	97.07	62.44	96.10	66.34	77.32	99.76	76.59	82.99
Leg [47]	95	65	65	85	85	95	95	65	81
HU [47]	85	65	65	65	65	85	75	65	71
Proposed approach	97.5	99.37	91.87	100	80.93	89.37	100	95	94.25

Table 3
Recognition rates for some different approaches.

Algorithm	Recognition rate (%)
Decision tree [43]	93.02
Robust symbolic representation [43]	89.03
Kernel-edit-distance [48]	91.33
Height functions [32]	88.72
IDSC+DP [36]	88.11
Fragment-based approach [43]	86.40
SC greedy [46]	86.40
PCA masks [46]	83.41
Legendre [47]	81
Proposed approach	94.25

presents the partitioning shape and the second one gives the obtained least squares curves.

5.1.2. Matching results

The experiments for shapes matching using the ETH-80 database can be grouped into three series. Fig. 5 shows some qualitative results on the performance of the proposed approach from the first series of tests. The left column represents the query shape. For each query, the top most similar shapes are depicted in every row. This figure shows that in most cases, the retrieved results belong to the same query class.
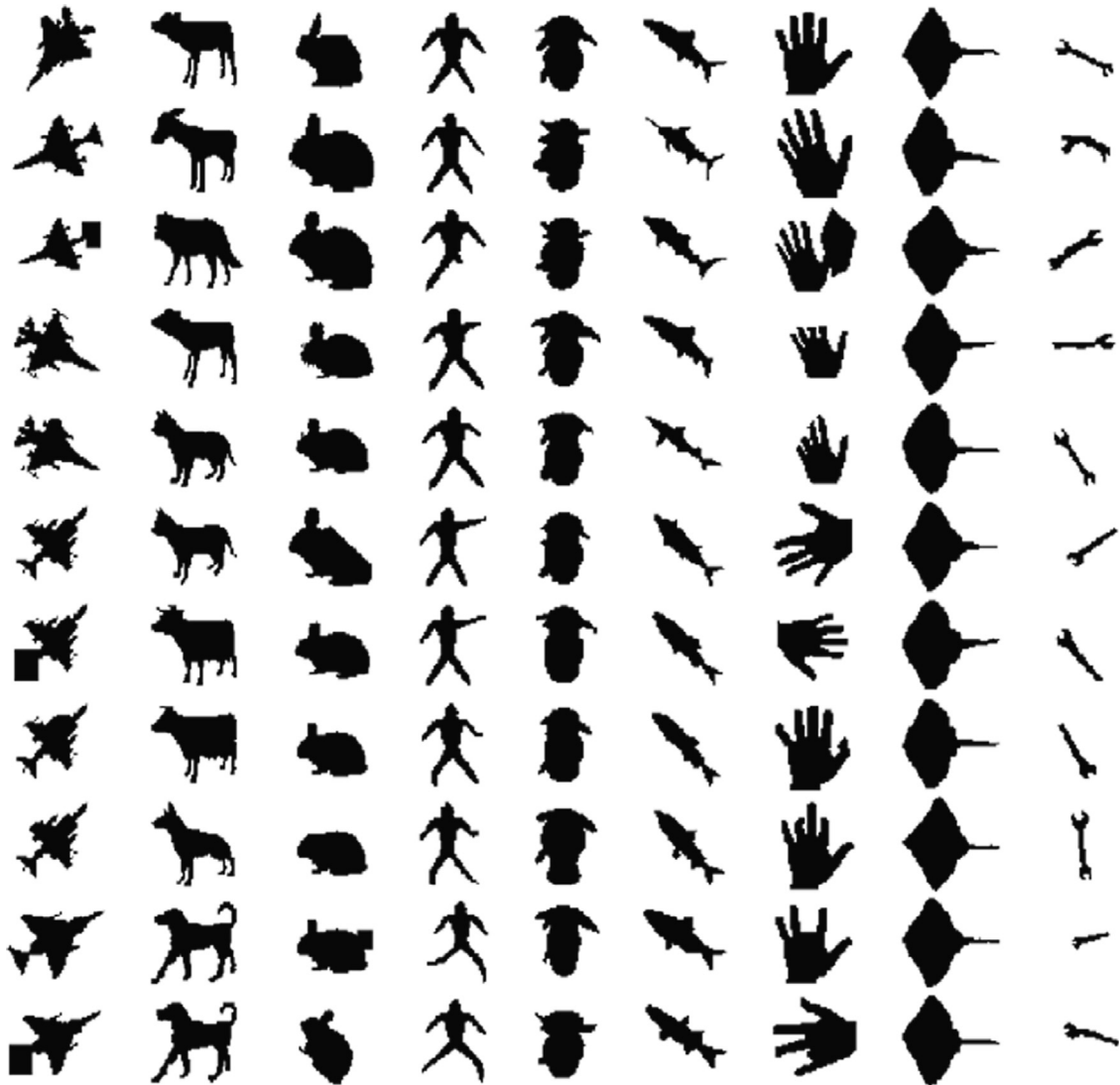
Fig. 9. Kimia-99 database.

Table 4
Retrieval results on the Kimia-99 database for some techniques in the literature.

Approaches	1st	2nd	3rd	4th	5th	6th	7th	8th	9th	10th	Total
Shape index [49]	43	51	58	52	52	49	51	47	45	44	492
ECCobj2D. s [49]	84	68	65	67	56	57	51	50	41	31	570
ECCobj2D. h [49]	87	74	66	64	49	52	45	38	33	33	541
HC [50]	96	84	78	77	78	65	68	58	60	48	712
Proposed approach	97	86	87	75	76	70	55	59	46	44	695
ECCobj2D [49]	94	85	81	73	81	73	64	59	56	35	701
Bernier and Landry [51]	97	94	92	85	74	73	65	54	43	36	713
Shape context [26]	97	91	88	85	84	77	75	66	56	37	756
Gen. model [52]	99	97	99	98	96	96	94	83	75	48	885
Shock edit [21]	99	99	99	98	98	97	96	95	93	82	956
IDSC [27]	99	99	99	98	98	97	97	98	94	79	958

The second series of tests are conducted to evaluate the performance of our system to scale change and rotation. For this purpose, we select some shapes randomly from the ETH-80 database. The selected shapes are scaled and rotated. Fig. 6 lists the retrieval results.

As can be seen in Fig. 6, the proposed approach possesses the important property of affine transformations.

Finally, in order to test the ability of the proposed approach to deal with the partial occluded shapes, some tests are performed with shapes partially occluded. These partial shapes, each consist of a portion of one database shape (see Fig. 7(a)). The seven shapes illustrated in Fig.7 (b) are used as test queries.
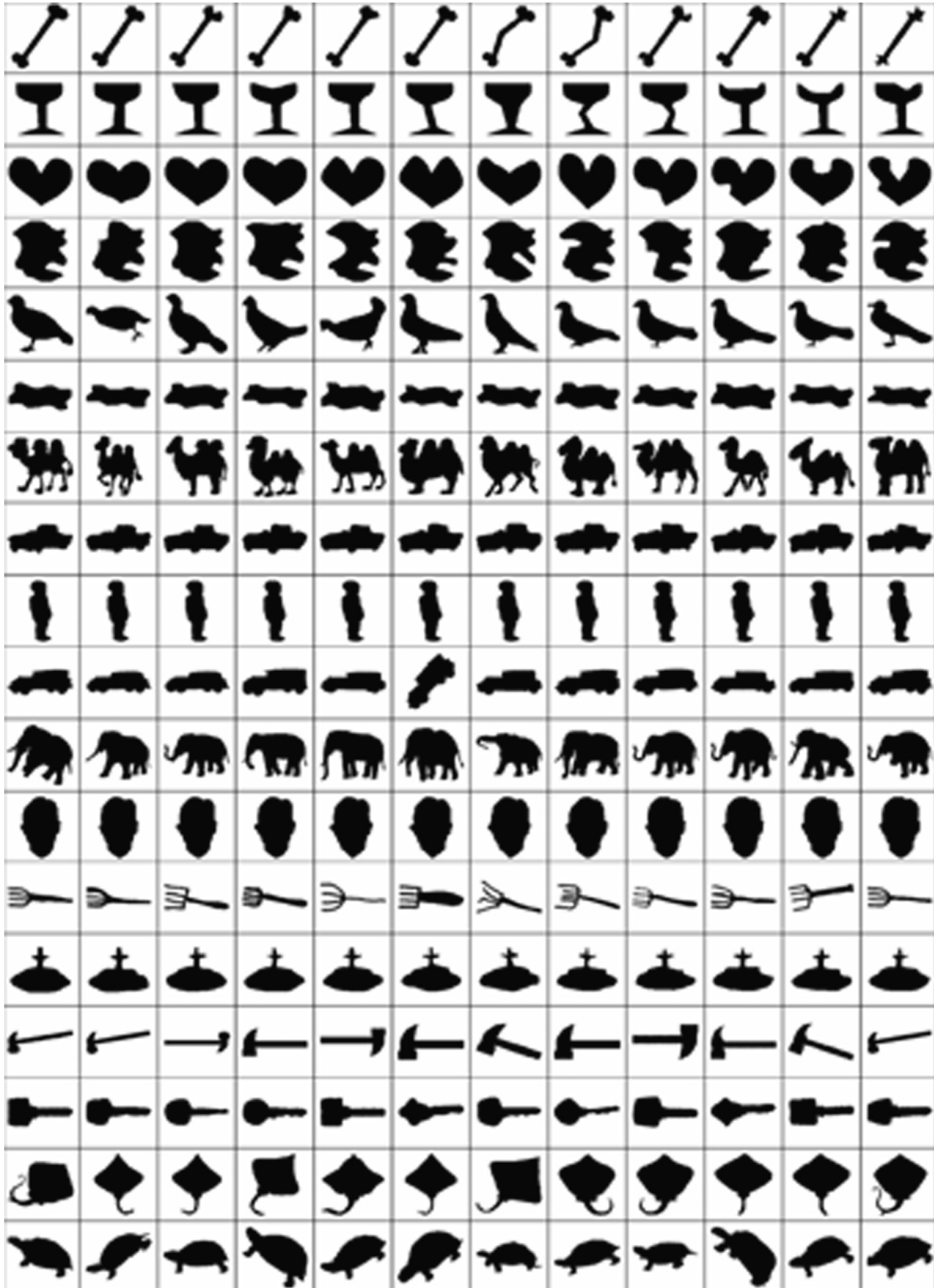
Fig. 10. Kimia-216 database.

For each query, the four most matched shapes retrieved by the proposed approach are shown in Fig. 8.

It can be observed from Fig. 8 that for different degrees of occlusion our algorithm can classify correctly most of the shape queries on occlusion. This is due to the use of the perceptual parts constituting the shape boundary. For the last two queries: the occluded apple is identified as a cup with a maximum score of similarity of 25% and the last one which is an occluded pear is classified as an apple with a maximum score of 14%. The mismatches are mainly due to the similarity between the parts constituting the shapes after occlusion. Our shape approach uses curves, so it is possible for different shapes to have some similar curves.
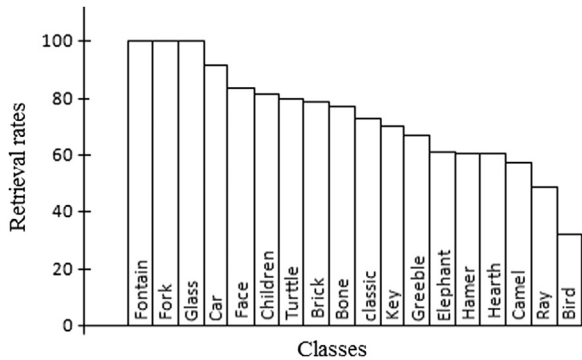
Fig. 11. Retrieval rates per class obtained by the proposed algorithm for the Kimia-216 database.

Table 5
Performance results using the precision at 10 measures.

Algorithm	Retrieval rate
CS	0.36
Fourier	0.37
MI	0.40
MS Fractal	0.62
SSD	0.72
SSD+GF	0.85
Proposed approach	0.64

Fig. 12. Some examples from MPEG-7 database.

5.1.3. Comparative study

In order to demonstrate the performance of our approach, a comparative study with some previous algorithms has been performed. The adopted test mode is the leave-one-object-out cross-validation. In each category, every shape is given as a query to the system. Recognition is considered successful if the correct category is assigned [43]. The final recognition rate is achieved by averaging over all test objects.

In Table 2, the average retrieval rates over the whole ETH-80 database for the proposed approach and some different methods are presented in the column "Average". The details of the recognition rates for each class are indicated in columns 2–9. From the experimentation summarized in this table, we observe that the largest recognition rate of 100% has been achieved for the classes cup and pear. For the shape classes apple, car and tomato the recognition rates are greater than 95%. This is due to the rough proposed description based on curves. On the other hand, as the proposed approach describes explicitly the significant parts constituting the outline shapes, it is possible for different shapes to have some similar curves and also the performance may decrease if the shape classes have some similarities as shown for the classes cow, dog and horse.

Table 3 below lists the recognition rate of our approach and some others algorithms reported for the ETH-80 database [46]. The proposed approach achieves a 94, 25% recognition rate; it is among the best proposed methods applied to this database and cited in [32,43].

5.2. Kimia-99 database

The Kimia-99 database consists of 99 shapes, grouped in 9 classes with 11 shapes in each class [21], as shown in Fig. 9. In this database, there are some visual transformations: occlusions, deformation and missing parts. In the experiment, each shape is used as a query and the first ten best matches, excluding the query, are retrieved.

The correct matches for each ranking position, over all 99 shapes are counted. A comparison of performances between some different approaches cited in [49] is shown in Table 4, summarizing the number of top 1–10 closest matches.

As shown in Table 4, our approach performs well relatively to recent methods [49,50]. Although the performance of our approach is lower than that of methods [21,27,26,51,52], our approach is simple and gives a rough description of shapes by taking into account only the boundary information.

5.3. Kimia-216 database

Kimia-216 provided by Sebastian et al. [21] consists of 216 shapes, grouped in 18 classes with 12 shapes in each class as shown in Fig. 10. In order to study the retrieval performance, all the 216 shapes have been considered as query shapes and the top 12 retrievals are recorded. The value 12 is chosen, as there are 12 shapes per class. Retrieval rate of 73.95% is achieved.

The retrieval rate per class is reported in Fig. 11.

As can be shown from Fig. 11, the proposed approach has the largest capability to retrieve relevant shapes of 100% for the classes Fork, Fountain and Glass. This result shows the ability of the proposed approach to retrieve shapes partially occluded, once most of the shapes in this database are partially occluded.

5.4. MPEG-7 database

The MPEG-7 database consists of 1400 shapes, grouped in 70 classes with 20 shapes in each class [53]. Fig. 12 shows some examples of these shapes. The performance of the proposed retrieval approach is compared with other methods in the literature: Contour Saliences Descriptor (CS),

Table 6
Performance results using the precision at 40 measures for MPEG-7.

Algorithm	Retrieval rate
CS [54]	0.31
Fourier [54]	0.30
MI [54]	0.38
MS Fractal [54]	0.54
SSD [54]	0.61
SC [55]	86.8
IDSC [55]	85.4
DDGM [55]	80.03
Planar graph cuts [55]	85
Triangle area [55]	87.23
Shape-tree [55]	87.7
ASC [55]	88.3
Layered graph [55]	88.75
Contour flexibility [55]	89.31
AIR [55]	93.67
Proposed approach	50.76
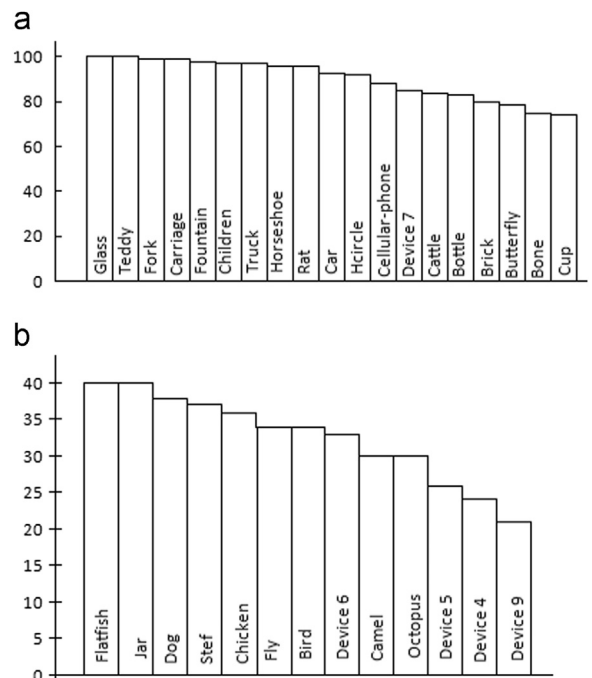
Fig. 13. Some retrieval rates per class for the MPEG-7 shape database.

Fourier, Moment Invariants (MI), Multi-scale Fractal Dimension, Shape Saliences (SSD) and shape saliences descriptor with global features. The comparative study is evaluated using the retrieval rate at 10 measures. Each shape is used as a query and the number of similar shapes which belong to the same class is counted in the top 10 matches.

Table 5 lists the reported results of these different approaches, cited in [54], on this database.

The second measure of accuracy used in our experimental evaluation is the normalized bull's-eye measure: each shape is used as a query and the number of similar shapes which belong to the same class are counted in the top 40 matches. This measure is used only for retrieval performance using the MPEG-7 database. Table 6 summarizes some results cited in [54,55].

We observe that the best descriptor is given by the AIR descriptor which combines different shape similarities [55]. Shape retrieval using MPEG-7 database is not a simple task, as there is a high similarity between shapes from different classes and visually dissimilarity in the same class. Note that the methods cited in [55] are contexts-based approaches and the proposed approach provides a different way of representing shapes based only on the curves constituting their boundaries.

Fig. 13 shows some retrieval rates per classe counting in top 10. Fig. 13(a) shows that the highest rate of 100% has been achieved for the classes Glass and Teddy. For the shape classes Face, Fork, Carriage, Fountain, Children, Truck, Horseshoe, Rat, Car and Hcircle the retrieval rate is greatest than 92.5%. On the other hand Fig. 13(b) shows some shape classes which have low rate.

This is due to that some shapes are visually similar to shapes of other classes. Furthermore, there are some shapes that are visually dissimilar from other shapes of their own class. As the proposed approach is based on different parts constituting the shape boundary, the performance may degrade if there is major similarity between shapes as can be seen by the examples illustrated below (see Fig. 14).
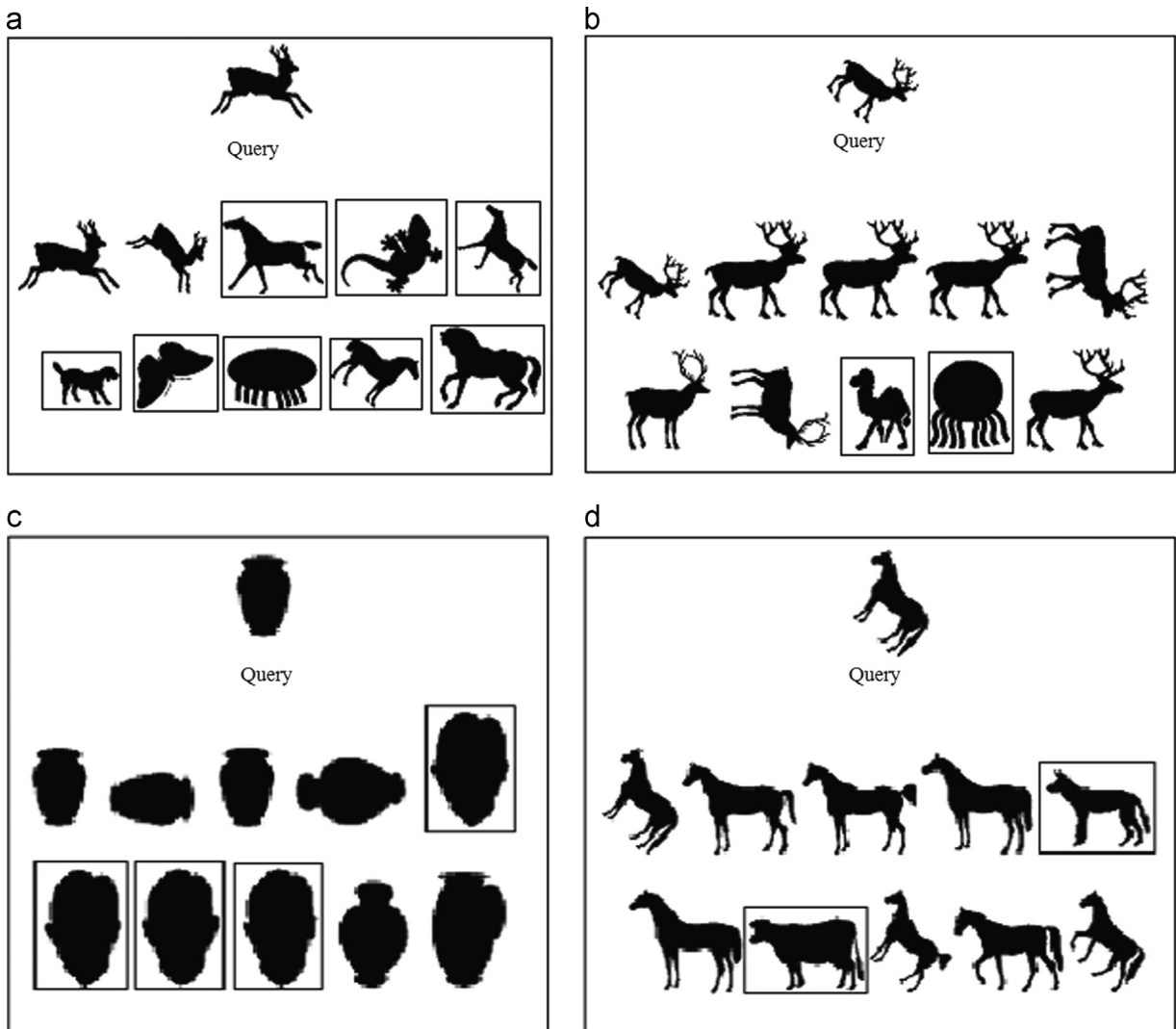
Fig. 14. Top 10 retrieval results for selected shape queries with mismatches: (a) and (b) Deer shapes, (c) Jar shape and (d) Horse shape.

Fig. 14 shows the top 10 retrieval results for Deer, Jar and Horse. It presents also the mismatches within top 10. The retrieved mismatches are enclosed by rectangular boxes. The shapes inside the box do not belong to the query class. The mismatches are due that our approach deals with the different curves constituting the shape boundary.

Regarding the application, this is not a bad result, since the shapes share some similar parts effectively, however considering that the performance evaluation considers only the shapes belonging to the same class as the shape query, the retrieval rate is penalized.

6. Conclusion

The goal of this paper is the description of two-dimensional objects based on the analysis of their boundaries. For this purpose, first the polygonal approximation is used in order to decompose the outline shape into a sequence of parts, second, the least squares model is applied to approximate each part by a polynomial curve. Finally the representation is transformed into invariant feature. The transformation is done by using distances from the shape's centroid to boundary. Based on the proposed shape similarity of normalized curves, our approach allows us to compute similarity measure between shapes. The experimental results on popular 2D shape matching benchmark databases show that the proposed approach is effective for shape matching and retrieval.

The obtained results have demonstrated invariance of our approach to some affine transformations such as rotation and scaling changes.

The use of an explicit description of different parts constituting the shape boundary enables our approach to overcome the partial occlusion.

Although the performance of the proposed approach is not the best one, it may be one of the most straightforward and feasible methods.

References

[1] D.S. Zhang, G.J. Lu, Review of shape representation and description techniques, Pattern Recognit. 37 (2) (2004) 1–19.
[2] W.Y. Kim, Y.S. Kim, A region-based shape descriptor using Zernike moments, Signal Process.: Image Commun. 16 (2000) 95–102.
[3] H.R. Boveiri, On pattern classification using statistical moments, Int. J. Signal Process. Image Process. Pattern Recognit. 3 (2010) 15–23.
[4] C.C. Lin, R. Chellappa, Classification of partial 2-D shapes using Fourier descriptors, IEEE Trans. Pattern Anal. Mach. Intell. 9 (1987) 686–690.
[5] R. EL-ghazal, O. Basir, S. Belkasim, Farthest point distance: a new shape signature for Fourier descriptors, Signal Process.: Image Commun. 24 (2009) 572–586.
[6] Y. Gdalyahu, D. Weinshall, Flexible syntactic matching of curves and its application to automatic hierarchical classification of silhouettes, IEEE Trans. Pattern Anal. Mach. Intell. 21 (1999) 1312–1328.
[7] G. McNeill, S. Vijayakumar, Hierarchical procrustes matching for shape retrieval, in: CVPR: Proceedings of the IEEE International Conference on Computer Vision and Pattern Recognition, 2006, pp. 885–894.
[8] S. Argawal, A. Awan, D. Roth, Learning to detect objects in images via a sparse Part-base representation, IEEE Trans. Pattern Anal. Mach. Intell. 26 (2004) 1475–1490.
[9] Y.W. Chen, C.L. Xu, Rolling penetrate descriptor for shape-based image retrieval and object recognition, Pattern Recognit. Lett. 30 (2009) 799–804.
[10] P.F. Felzenszwalb, J. Schwartz, Hierarchical matching of deformable shapes, in: CVPR: Proceedings of the IEEE International Conf on Computer Vision and Pattern Recognition, 2007, pp. 1–8.
[11] S.K. Hwang, W.Y. Kim, A novel approach to the fast computation of Zernike moments, Pattern Recognit. 39 (2006) 2065–2076.
[12] C.S. Pooja, Improving image retrieval using combined features of Hough transform and Zernike moments, Opt. Lasers Eng. 49 (2011) 1384–1396.
[13] G.Y. Yang, H.Z. Shu, C. Toumoulin, G.N. Han, L.M. Luo, Efficient Legendre moments computation for grey level images, Pattern Recognit. 39 (2006) 74–80.
[14] CH. Srinivasa Rao, S. Srinivas Kumar, B. Chandra Mohan, Content based retrieval using Legendre moments and support vector machine, Int. J. Multimed. Appl. 2 (2010) 69–79.
[15] D Zhang, G. Lu, Shape-based image retrieval using generic Fourier descriptor, Signal Process.: Image Commun. 17 (2002) 825–848.
[16] H. Sahbi, Kernel PCA for similarity invariant shape recognition, Neurocomputing 70 (2007) 3034–3045.
[17] H. Freeman, Computer processing of line-drawing images, Comput. Surv. 6 (1974) 57–97.
[18] E. Arkin, L. Chew, D. Huttenlocher, J. Mitchell, An efficient computable metric for comparing polygonal shapes, IEEE Trans. Pattern Anal. Mach. Intell. 13 (1991) 209–216.
[19] A. Carmona-poyato, F.J. Madrid-Cuevas, R. Medina-Carnicer, R. Munoz-Salinas, Polygonal approximation of digital planar curves through break point suppression, Pattern Recognit. 43 (2010) 14–25.
[20] H. Blum, A transformation for extracting new descriptors of shape, Models for the Perception of Speech and Visual Form, MIT Press, Cambridge, 1967, 362–380.
[21] T.B. Sebastian, P.N. Klein, B.B. Kimia, Recognition of shapes by editing their shock graphs, IEEE Trans. Pattern Anal. Mach. Intell. 26 (2004) 550–571.
[22] E. Petrakis, E. Milios, Shape retrieval based on dynamic programming, IEEE Trans. Image Process. 9 (2000) 141–147.
[23] F. Mokhtarian, S. Abbasi,J. Kittler, Efficient and robust retrieval by shape content through curvature scale space, in: A.W.M. Smeulders, R. Jain (Eds.), Image Databases and Multi-Media Search, 1996, pp. 51–58.
[24] S. Escalera, A Fornés, O Pujol, P Radeva, G Sanchez, J. Liados, Blurred shape model for binary and grey-level symbol recognition, Pattern Recognit. Lett. 30 (2009) 1424–1433.
[25] F. Fotopoulou, G. Economou, Multivariate angle scale descriptor for shape retrieval, in: Proceedings of SPAMEC, Cluj-Napoca, Romania, 2011, pp. 105–108.
[26] N. Alajlan, I.E. Rube, M.S. Kamel, G. Freeman, Shape retrieval using triangle area representation and dynamic space warping, Pattern Recognit. 40 (2007) 1911–1920.
[27] K. Kpalma, J. Ronsin, Turning angle based representation for planar objects, IEE Electron. Lett. 43 (2007) 561–563.
[28] K. Kpalma, C. Bai, M. Chikr el mezouar, K. Belloulata, N. Taleb, L. Belhallouche, D. Boukerroui, A new histogram-based descriptor for images retrieval from databases, in: International Workshop on Next Generation Intelligent Medical Decision Support Systems, Sofia, Bulgaria, 2012.
[29] D. Paglieroni, A.K. Jain, A Control point theory for boundary representation and matching, in: Proceedings of ICASSP, 1985, pp. 1851–1854.
[30] N. Laiche, Geometric description of outline shapes and recognition, in: Proceedings of the IADIS International Conference Computer Graphics, Visualization, Computer Vision and Image Processing, Freiburg, Germany, July 2010, pp. 526–528.
[31] H. Liu, L.J. Latecki, W. Liu, A unified curvature definition for regular, polygonal, and digital planar curvatures, Int. J. Comput. Vis. 80 (2008) 104–124.
[32] J. Wang, X. Bai, X. You, W. Liu, L.J. Latecki, Shape matching and classification using height functions, Pattern Recognit. Lett. 33 (2012) 134–143.
[33] S. Belongie, J. Malik, J. Puzicha, Shape matching and object recognition using shape contexts, IEEE Trans. Pattern Anal. Mach. Intell. 24 (2002) 509–522.
[34] H. Ling, D. Jacobs, Shape classification using the inner- distance, IEE Trans. Pattern Anal. Mach. Intell. 29 (2007) 286–299.
[35] L. Nanni, S. Braham, A. Lumini, Local phase quantization descriptor for improving shape retrieval/classification, Pattern Recognit. Lett. 33 (2012) 2254–2260.
[36] R.X. Hu, W. Jia, D. Zhang, J. Gui, L.T. Song, Hand shape recognition based on coherent distance shape contexts, Pattern Recognit. 45 (2012) 3348–3359.
[37] C.J. Wu, J.Z. Liu, X. Tang, 2D shape matching by contour flexibility, IEEE Trans. Pattern Anal. Mach.Intell. 31 (2009) 180–186.

[38] K. Shoji, Generalized skeleton representation and adaptive rectangular decomposition of Binary images, in: P.D. Gader, E.R. Dougherty, J.C. Serra (Eds.), SPIE Proceedings of Image Algebra and Morphological Image Processing III, 1992, pp. 404–415.

[39] S. Berriti, A.D. Bimbo, P. Pala, Retrieval by shape similarity with perceptual distance and effective indexing, IEEE Trans. Multimed. 2 (2000).

[40] C. Di Ruberto, L. Cinque, Decomposition of two-dimensional shapes for efficient retrieval 27 (2009) 1079–1107Image Vis. Comput. 27 (2009) 1079–1107.

[41] L.J. Latecki, V. Megalooikonomou, Q.A. Wang, D. Yu, An elastic partial shape matching technique, Pattern Recognit. 40 (2007) 3069–3080.

[42] M. Cui, J. Femiani, J. Hu, P. Wonka, A. Razdan, Curve matching for open 2-D curves, Pattern Recognit. Lett. 33 (2009) 1–10.

[43] M.R. Daliri, V. Torre, Classification of silhouettes using contour fragments, Comput. Vis. Image Underst. 113 (2010) 1017–1025.

[44] D. Kirk, D. Voorhies, The rending architecture of the DN0000VS, Comput. Graph. 24 (4) (1990) 299–307.

[45] J. Philip, D. Schneider, H. Eberly, Geometric tools for computer graphics, Textbook Binding, 2002.

[46] B. Leibe, B. Scheille, Analysing appearance and contour based methods for object categorization, in: Proceedimgs of the International Conference on Computer Vision and Pattern Recognition, Madison,Wisconsin, 2003.

[47] T. Arif, S. Zyad Shaaban, L. Krekor, S. Baba, Object classification via geometrical, Zernike and Legendre moments, J. Theor. Appl. Inf. Technol. 7 (11) (2009) 31–37.

[48] M.R. Daliri, V Torre, Shape recognition based on Kernel-edit distance, Comput. Vis. Image Underst. 114 (2010) 1097–1103.

[49] A. Ion, N.M. Artner, G. Peyré, W.G. Kropatsch, L.D. Cohen, Matching 2D and 3D articulated shapes using the eccentricity transform, Comput. Vis. Image Underst. 115 (2011) 817–834.

[50] Y. Ebrahim, M. Ahmed, W. Abdelsalam, S.C. Chau, Shape representation and description using the Hilbert curve, Pattern Recognit. Lett. 30 (2009) 348–358.

[51] T. Bernier, J.A. Landry, A new method for representing and matching shapes of natural objects, Pattern Recognit. 36 (2003) 1711–1723.

[52] Z. Tu, A.L. Yuille, Shape matching and recognition using generative models and informative features, in: Proceedings of the 8th European conference on computer vision, ECCV Prague, Czech republic, 2004.

[53] L.J. Latecki, R. Lakamper, Shape similarity measure based on correspondence of visual parts, IEEE Trans. Pattern Anal. Mach. Intell. 22 (10) (2000) 1182–1190.

[54] G.V. Pedrosa, M.A. Batista, C.A.Z. Barcelos, Image feature descriptor based on shape salience points, Neurocomputing 120 (2013) 156–163.

[55] X. Bai, B. Wang, C. Yao, W. Liu, Z. Tu, O-transduction for shape retrieval, IEEE Trans Image Process. 21 (5) (2012) 2747–2757.